Reprinted with permission from: Prosperi-Porta G, Kedzior S, Muirhead B, Sheardown H. Phenylboronic-Acid-Based Polymeric Micelles for Mucoadhesive Biomacromolecules 2016, 17, 1449−1457 DOI: 10.1021/acs.biomac.6b00054

Phenylboronic-Acid-Based Polymeric Micelles for Mucoadhesive Anterior Segment Ocular Drug Delivery

Graeme Prosperi-Porta,[†,§] Stephanie Kedzior,[‡] Benjamin Muirhead,[†] and Heather Sheardown*[,†,‡]

[†]School of Biomedical Engineering, McMaster University, Main Street West, Hamilton, Ontario L8S 4L8, Canada [‡]Department of Chemical Engineering, McMaster University, 1280 Main Street West, Hamilton, Ontario L8S 4L8, Canada

Topical drug delivery to the front of the eye is extremely inefficient due to effective natural protection mechanisms such as precorneal tear turnover and the relative impermeability of the cornea and sclera tissues. This causes low ocular drug bioavailability, requiring large frequent doses that result in high systemic exposure and side effects. Mucoadhesive drug delivery systems have the potential to improve topical drug delivery by increasing pharmaceutical bioavailability on the anterior eye surface. We report the synthesis and characterization of a series of poly(L-lactide)-b-poly(methacrylic acid-co-3-acrylamidophenylboronic acid) block copolymer micelles for use as mucoadhesive drug delivery vehicles. Micelle properties, drug release rates, and mucoadhesion were shown to depend on phenylboronic acid content. The micelles showed low in vitro cytotoxicity against human corneal epithelial cells and undetectable acute in vivo ocular irritation in Sprague–Dawley rats, suggesting good biocompatibility with the corneal surface. The micelles show the potential to significantly improve the bioavailability of topically applied ophthalmic drugs, which could reduce dosage, frequency of administration, and unintentional systemic exposure. This would greatly improve the delivery of the ocular drugs such as the potent immunosuppressive cyclosporine A used in the treatment of severe dry eye disease.

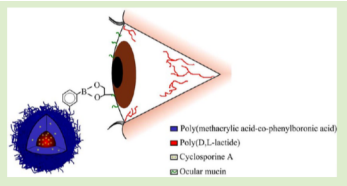

INTRODUCTION

The most common method to treat anterior segment diseases of the eye is by topical drop administration due to its low cost, ease of application, and noninvasiveness. Unfortunately, numerous barriers prevent efficient delivery of therapeutics to the anterior segment resulting in <5% of the administered dose reaching the anterior tissues.[1] Static barriers including tight junctions of the conjunctiva, the alternating hydrophobic corneal epithelium and hydrophilic corneal stroma, and dynamic barriers including the rapid tear turnover and the vasculature and lymphatics of the conjunctiva all contribute to the highly impenetrable anterior surface.[1,2] Precorneal clearance mechanisms such as blinking, rapid tear turnover, and lacrimal drainage are additional physiological barriers that must be overcome to achieve effective drug delivery. Upon instillation of an eye drop, the maximal 30 μL that can be held in the cul-de- sac is restored to its normal 7 uL tear volume within 2 to 3 min, resulting in the rapid drainage of 80% or more drug through the nasolacrimal duct, leading to systemic absorption and potential adverse side effects.[1,3]

The tear film itself is composed of an outer lipid layer, a middle aqueous layer containing secreted mucin, and an inner mucin layer immobilized on a glycocalyx covering the corneal and conjunctival epithelium.[4,5] The inner immobilized mucin layer, in addition to providing an interface between the aqueous and corneal epithelial layers, is thought to act as yet another protective barrier against the diffusion of macromolecules, microbes, and hydrophobic molecules due to its hydrophilic nature.[5] Rose bengal, an anionic dye, has been shown to stain corneal epithelium more readily with less mucin, suggesting that it may also act as an additional barrier.[6]

One method that has been explored to improve drug transport into the ocular tissues has been to utilize mucoadhesive polymers that increase the bioavailability of drug in the immobilized mucin layer. There are many well- known natural mucoadhesive polymers including chitosan,[7–9] polysaccharides,[10–12] thiomers,[13,14] and many others, but these materials generally lack the versatility for nanoparticle design to achieve desirable release characteristics. Phenylboronic acid (PBA) is a synthetic molecule that has been extensively used in glucose sensing and insulin delivery systems due to its ability to form high-affinity complexes with 1,2-cis-diols.[15] This affinity between boronic acids and diols has also been utilized in other mucoadhesive drug delivery systems such as vaginal delivery of interferon,[16] nasal delivery of insulin,[17,18] and ocular delivery of cyclosporine A (CycA).[19]

Dry eye disease (DED) is one of the most frequent ocular illnesses in the United States with approximately 4.3% of men and 7.8% of women over the age of 50 showing dry eye symptoms.[20,21] On the basis of the Salisbury eye study, the prevalence of DED in elderly Americans aged 65–84 increases to over 14%.[22,23] DED is a multifactorial disease that

can be caused by any combination of insufficient tear production and evaporative loss resulting in ocular burning, stinging, foreign body sensation, visual disturbance, inflammation, and potential damage to the ocular surface.[24] CycA, commercially available as Restasis (0.05% CycA ophthalmic emulsion) for the treatment of DED, is a non-water-soluble cyclic peptide.[25] CycA is a potent immunosuppressive agent that has been shown to improve DED by reducing lymphocyte activation, which reduces the production of inflammatory substances that can lead to tissue damage,[26,27] and by increasing the number of goblet cells, which are responsible for the secretion of lubricious mucin.[28]

We have developed a series of mucoadhesive block copolymer micelles based on phenylboronic acid using reversible addition–fragmentation chain transfer polymerization (RAFT) capable of targeted delivery of CycA to the ocular mucosa. The synthesis, chemical, and biological characterization of these micelles for mucoadhesive drug delivery to the anterior segment will be discussed herein.

EXPERIMENTAL SECTION

Materials. Unless otherwise stated, all materials were purchased from Sigma-Aldrich (Oakville, ON) and used as received. 3- Acrylamidophenylboronic acid was purified by recrystallization in purified water. Azobis(isobutyronitrile) (AIBN) was purified by recrystallization in methanol. 1,4-Dioxane, tetrahydrofuran, diethyl ether, and acetonitrile were purchased from Caledon Laboratories (Caledon, ON) and used as received. DMSO-d_6 was purchased from Cambridge Isotope Laboratories (Andover, MA) and used as received. Purified water with a resistivity of 18.2 MΩ cm was prepared using a Milli-pore Barnstead water purification system (Graham, NC). Phosphate-buffered saline (PBS) was purchased from BioShop (Burlington, ON). Cellulose dialysis membranes with molecular weight cutoff (MWCO) values of 3.5 and 50 kDa were purchased from Spectrum Laboratories (Rancho Dominguez, CA). 3-[4,5- Dimethylthiazol-2-yl]-2,5-diphenyl-tetrazolium bromide (MTT), Cal- cein AM, and ethidium bromide were purchased from Life Technologies (Carlsbad, CA) and were used as received.

Synthesis and Characterization of pLA-b-p(MAA-PBA) Copolymers. pLA-b-p(MAA-PBA) (LMP) copolymers were synthe- sized by RAFT polymerization. In a typical reaction procedure (80:20:1.4:0.2 molar feed ratio of MAA/PBA/pLA/AIBN), meth- acrylic acid (MAA; 192.9 mg, 2.24 mmol), PBA (107.1 mg, 0.56 mmol), poly(D,L-lactide) 4-cyano-4-[(dodecylsulfanylthiocarbonyl)- sulfanyl]pentoate (pLA-CDP; 200.0 mg, 0.04 mmol), and AIBN (1.10 mg, 0.01 mmol) were dissolved in 5 mL of 90:10 1,4-dioxane/ water to form a 10% (w/v) solution. The solution was degassed by performing three freeze–pump–thaw cycles, followed by replacement of the atmosphere with dry nitrogen. The flask was then heated to 70 °C for 24 h under constant stirring. This copolymer, denoted LMP-20 (20 wt % PBA in the poly(MAA-co-PBA) block), was isolated by precipitation into 10 times excess of cold anhydrous diethyl ether and further purified by repeated precipitation into diethyl ether from tetrahydrofuran two additional times. The copolymer was dried in a vacuum oven at 50 °C for 24 h before further use.

LMP copolymer composition and molecular weight were determined using proton nuclear

magnetic resonance (^{1}H NMR; Bruker AV 600) in DMSO-d_6. Additionally, LMP polymerization kinetics were studied in the LMP-10 copolymer to determine the distribution of PBA within MAA-PBA block and controlled nature of polymerization. Polymerization was performed as previously stated, although at specified time points a dry-nitrogen-purged airtight needle was used to remove 50 μL samples for ^{1}H NMR.

Micelle Formation and Characterization. Micelles were formed by precipitation into purified water from acetone. In brief, 20 mg of LMP copolymer was dissolved in 2 mL of acetone and then added dropwise to 6 mL of purified water under constant stirring through a 30 G needle at a rate of 0.5 mL min^{-1} using a syringe pump. The acetone/water solutions were then allowed to stir uncovered at room temperature for 48 h to evaporate the acetone before subsequent use. The micelle concentration was adjusted by dilution with purified water or further evaporation prior to characterization.

Micelle size was determined using dynamic light scattering (Zetasizer Nano S, Malvern). In brief, micelles were diluted to a final concentration of 0.25 mg mL^{-1} at pH 7.4 in 0.1 M PBS to simulate physiological conditions, and the z-average diameter and dispersity were measured. Dry micelle size and shape were confirmed using a Jeol JEM-1200EX transmission electron microscope with an 80 kV electron beam. TEM samples were prepared by air-drying 4 μL of 50 μg mL^{-1} micelle solution on a 200 mesh Formvar-coated copper grid. Micelle colloidal stability was assessed using zeta potential (ZetaPlus Analyzer, Brookhaven). Zeta potential was measured at micelle concentrations of 1 mg mL^{-1} in pH 7.4 0.1 M PBS.

The critical micelle concentration (CMC) was determined using the pyrene fluorescent probe method.[29] A predetermined amount of pyrene was dissolved in acetone and added to 2 mL vials and allowed to evaporate. Micelle solutions ranging from 10 to 10^{-5} mg mL^{-1} were added and incubated for 24 h at room temperature, resulting in final pyrene concentrations of 6.0×10^{-7} mol L^{-1}. Fluorescence was measured using a TECANM1000 Proplatereader(Man¨nedorf, Switzerland). The emission spectrum was measured from 350 to 470 nm with a step size of 1 nm after an excitation wavelength of 340 nm. The CMC was determined by plotting the intensity ratio of peaks at 373 nm to those at 383 nm against the logarithm of concentration. The emission and excitation bandwidths for all measurements was 5 nm.

Mucoadhesion by Surface Plasmon Resonance. Mucoadhe- sion was determined using surface plasmon resonance (SPR; SPR Navi 200, BioNavis). In brief, SPR102-AU gold sensors were cleaned using piranha (3:1 94% sulfuric acid/hydrogen peroxide), rinsed extensively with purified water, and dried under a stream of nitrogen. The sensor surfaces were then incubated in 100 μL of 100 μg mL^{-1} bovine submaxillary gland mucin for 24 h at 20 °C and then rinsed with purified water to remove any mucin that was not physically bound. SPR measurements were conducted by flowing simulated tear fluid (STF; 23.1 mM KCl, 20.0 mM $NaHCO_3$, 1 mM $CaCl_2 \cdot 2H_2O$, 113.5 mM NaCl; pH 7.4) for 10 min to achieve a stable baseline. The solution was then changed to a 1 mg mL^{-1} solution of chitosan or LMP micelles for 50 min. At this point, the solution was changed back to simulated tear fluid to assess mucoadhesive stability. All measurements were conducted at a flow rate of 50 μL min^{-1}, a temperature of 22 °C, and a fixed angle scan of 65.4°.

Cyclosporine A Release. CycA release from micelles was determined using high-performance liquid chromatography (HPLC). Twenty mg of the LMP copolymer was dissolved in 2 mL of acetone containing 1.5 mg mL^{-1} CycA. This solution was added dropwise to 6 mL of purified water. The solution was left under stirring for 24 h to evaporate the acetone, and the volume was readjusted to 6 mL with purified water. 0.5 mL was removed and filtered with Nanosep 10K Omega centrifugal units (10 kDa MWCO, Pall Corporation) to separate micelles from free CycA. The filtrate was collected to determine entrapment efficiency (EE). Five mL of noncentrifuged sample was then added to 50 kDa MWCO dialysis tubes, placed in 15 mL of STF, and added to a reciprocating shaker bath (VWR 1217 reciprocating bath; 32 °C, 30 rpm) to improve mixing. CycA release from micelles was compared with blank CycA prepared the same way but not containing any LMP copolymer. At specified time points, 2.5 mL samples were removed and replaced with fresh prewarmed STF. These samples were analyzed using a Waters HPLC consisting of a 2707 autosampler, 2489 UV spectrophotometer, 1525 binary HPLC pump, Atlantis dC18 5 μm 4.6 × 100 mm column, and Breeze 2 software (Build 2154). A 0.7 mL min^{-1} isocratic flow rate of 80:20 acetonitrile/0.1% trifluoroacetic acid in purified water as the mobile phase, a 60 °C column temperature, a 20 μL sample injection volume, and a 210 nm detection wavelength were used. Sample concentrations were determined based on a standard calibration curve of CycA in the mobile phase.

Cell Culture. For cell culture, all copolymers were extensively dialyzed in 2:1 acetone/water solutions against 3.5 kDa MWCO dialysis tubing to remove any water-insoluble impurities, followed by the transition to purified water, followed by lyophilization. 50 mg of copolymer was then dissolved in 1 mL of acetone and added dropwise under constant stirring to 2.5 mL of sterile water. The acetone was allowed to evaporate for 48 h under constant stirring, the volume was adjusted, and dilutions were performed to achieve 20 and 4 mg mL^{-1} micelle concentrations. Concentrated PBS and penicillin/streptomycin were added to these solutions to achieve final concentrations of 0.1 M and 1% (v/v). respectively. Human corneal epithelial cells (HCECs) were cultured in keratinocyte serum-free media (KSFM) supple- mented with bovine pituitary extract (0.05 mg mL^{-1}) and epidermal growth factor (0.005 mg mL^{1}). HCECs were seeded in 96-well plates at densities of 5000 cells $well^{-1}$ and incubated in a temperature- controlled CO_2 incubator (37 °C, 5% CO_2, 95% air, 100% humidity). After 24 h of growth the media was replaced with 150 μL of KSFM and50μLofPBS,50μLof4mgmL^{-1} LMPmicelles,or50μLof20 mg mL^{-1} micelles for final LMP micelle concentration of 0, 1, and 5 mg mL^{-1}. The plates were incubated for 24 and 72 h, at which point cell viability was assessed using an MTT assay and live/dead cell counts were determined by a calcein AM (CalAM)/ethidium homodimer-1 (EthD-1) assay (n = 6 used for all assays). % viability and % morbidity were determined by spectrophotometric analysis (TECAN M200 infinite pro) based on the ratio of the absorbance (MTT) or fluorescence (CalAM/EthD-1) in wells containing micelles compared with control wells. Fluorescence images were collected with an Olympus IX51 inverted fluorescence microscope.

In Vivo Ocular Irritation. Micelles were prepared and purified as previously described. The volume was then adjusted to achieve a final concentration of 5 mg mL^{-1}. Finally, the pH of the micelle solution was adjusted to 7.6 using PBS to match that of the precorneal tear film.[30] Ocular irritancy was determined by applying 10 μL of the LMP- 0, LMP-10, and LMP-30 solution to the

right eye of 4 month old Sprague–Dawley rats (Charles River, strain code 400) once per day for a total of 10 days. Treated eyes were held shut and gently massaged for several seconds to ensure proper dispersal over the ocular surface. At the end of this test period, eyes were examined with slit lamp microscopy (Phoenix Micron IV) and optical coherence tomography (OCT; Phoenix Micron IV). Fluorescein staining was performed using ophthalmic Amcon Fluorescein Glostrips. Corneas were examined qualitatively for any abnormalities, inflammation, or material–host interaction.

Animal Studies. All animals were handled according to the principles of the ARVO Statement for the Use of Animals in Vision Research as well as the guidelines set out by the Animal Research Ethics Board at McMaster University.

Statistical Analysis. A one-factor analysis of variance (ANOVA) was used to analyze the zeta potential, micelle diameter, and HCEC viability using $\alpha = 0.05$ with Tukey post hoc. Statistical analysis was performed using IBM SPSS Statistics V22.0 statistical software (IBM, Armonk, NY). All error bars represent standard deviation.

RESULTS AND DISCUSSION

Copolymer Characterization. Scheme 1 shows the general reaction scheme for RAFT polymerization used to synthesize the LMP block copolymer. ^{1}H NMR was used to determine the molar composition and the number-average molecular weight of the LMP copolymers based on monomer conversion. Table 1 shows the final copolymer compositions and molecular weights. These results consistently showed that MAA achieved higher conversions of 0.8 to 0.89 compared with PBA that only achieved conversions of 0.6 to 0.65 after 24 h. To understand the effect of polymerization kinetics on the distribution of PBA and MMA, we performed a kinetic study on the LMP-10 copolymer. The results, shown in Figure 1, demonstrate that MAA has a higher polymerization rate, which causes the monomer to be consumed more quickly, allowing the PBA monomer to preferentially polymerize during the later stages of the reaction. This leads to two results: the final overall copolymer composition has a higher total MAA/PBA ratio than the feed ratio and the instantaneous distribution of PBA increases over the course of polymerization to produce a poly(MAA-co-PBA) gradient. The PBA gradient may be beneficial to improving mucoadhesion because the PBA polymerizes in higher density at the end of the chain, which may be sterically forced to reside on the micelle surface facilitating mucoadhesion.

Scheme 1. Reversible Addition–Fragmentation Chain Transfer Polymerization Reaction Mechanism Used to Synthesize the LMP Block Copolymers

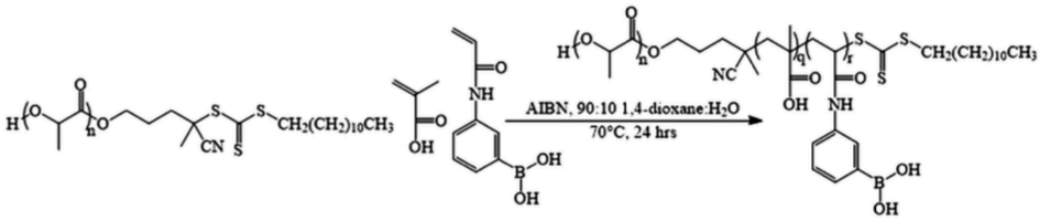

Table 1. LMP Block Copolymer Polymerization Data[a]

	molar feed ratio (pLA-CDP/MAA/PBA)	xMAA	xPBA	final composition (pLA/pMAA/pPBA)	M_n (kDa)
pLA-CDP				100:0:0	4.7
LMP-0	44.3:55.7:0	0.80		49.8:50.2:0	10.4
LMP-5	45.8:51.5:2.7	0.88	0.65	49.4:49.6:1.9	10.7
LMP-10	47.2:47.5:5.3	0.87	0.66	51.3:46.7:3.8	10.6
LMP-20	49.8:40.2:10.0	0.89	0.68	53.9:41.7:7.4	10.5
LMP-30	52.1:33.5:14.4	0.84	0.65	58.1:35.2:10.4	10.0

[a]Composition in mol %, conversion, and molecular weight were determined by ^{1}H NMR.

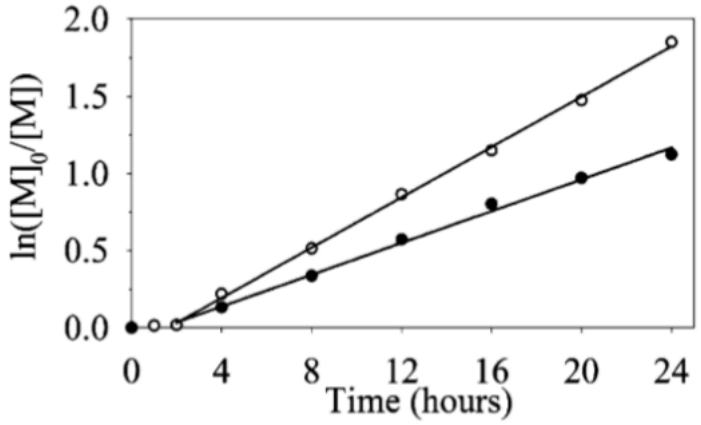

Figure 1. Polymerization kinetics of MAA (○) and PBA (●) in the LMP-10 copolymer synthesis showing distinct linear rates of polymerization.

Because of the amphiphilic properties of the LMP copolymer and the high affinity of unprotected phenylboronic acid to the column, gel permeation chromatography did not give accurate molecular weights or dispersity. Instead, average molecular weight was calculated based on conversion using ^{1}H NMR. The kinetic study was also used to assess the living nature of the polymerization reaction. After an initial lag period a linear relationship between the natural logarithm of $[M]_o/[M]$ was found, which is expected for well-controlled RAFT polymerization. This suggests that the dispersity will in fact be low due to the controlled nature of this polymerization.

Micelle Characterization. DLS was used to determine the z-average diameter and dispersity of the LMP micelles, shown in Table 2. The results indicate a trend between

the PBA content and the micelle size. Micelles containing higher PBA content show a higher z-average diameter by DLS. We had expected increasing hydrophobic PBA in the micelle to result in more compact particles due to decreased water content in the corona and increased interactions with the hydrophobic poly(D,L-lactide) core; however, the DLS dispersity results suggest that increased PBA in the corona also increases the hydrophobic interactions between micelles, resulting in agglomeration that leads to a larger apparent diameter. Interestingly, the LMP-0/5/10 micelles loaded with CycA did not show significant changes in micelle diameter ($p > 0.05$), but the LMP-20/30 micelles showed significant decreases in micelle diameter (both had $p < 0.01$). The CycA loading may interact with the hydrophobic PBA and poly(D,L-lactide) segments in these micelles, reducing the inter- and intramolecular interactions that cause the formation of larger diameter micelles.

Table 2. LMP Block Copolymer Micelle Diameter Determined Using DLS[a]

	unloaded micelles		CycA-loaded micelles	
	diameter ± SD (nm)	dispersity	diameter ± SD (nm)	dispersity
LMP-0	36 ± 0.6	0.15	36 ± 1.0	0.13
LMP-5	37 ± 0.6	0.18	40 ± 1.3	0.15
LMP-10	43 ± 1.4	0.15	45 ± 0.2	0.14
LMP-20	59 ± 2.9	0.29	44 ± 3.8	0.34
LMP-30	64 ± 3.4	0.26	50 ± 5.7	0.33

[a]All measurements are reported as diameter ± SD of three runs in nanometers.

To confirm the size and morphology TEM was performed on the non CycA loaded micelles, shown in Figure 2. All images showed spherical morphologies, suggesting micelle formation with dry diameters smaller than those determined by DLS. At the low concentration used to prepare TEM samples it is unlikely that substantial agglomerates could be seen.

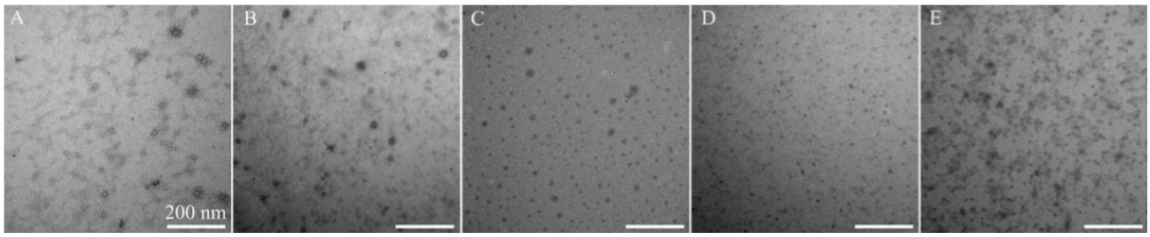

Figure 2. Transmission electron micrograph of LMP copolymer micelles. Scale bar represents 200 nm in all images (A) LMP-0, (B) LMP-5, (C) LMP-10, (D) LMP-20, and (E) LMP-30. All copolymer micelles show a morphology indicative of spherical micelles.

Zeta potential measurements were performed to determine the colloidal stability of the LMP micelles. The results in Figure 3 show increasing surface charge with increasing PBA content. This trend was unexpected because these measurements were performed in 0.1 M PBS at pH 7.4, above the pK_a of MAA but below the pK_a of PBA, which would cause most MAA groups to be deprotonated and most PBA groups to be uncharged; however, the increased zeta potential with increasing PBA content can be explained by an

increased surface charge density; the increasing hydrophobic PBA in the micelle's corona causes increased hydrophobic interactions between polymer chains, creating a more densely packed corona with a lower water content. The increased PBA content facilitates closer packing of charges on the micelle's surface, creating an increased charge density on the micelle surface.

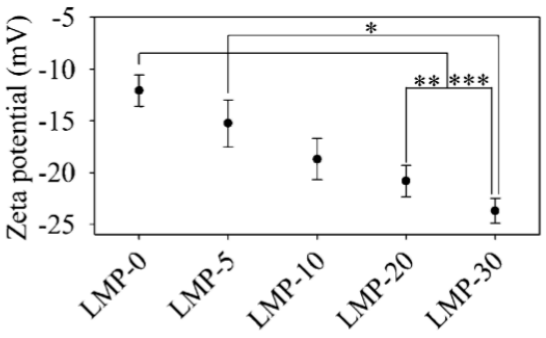

Figure 3. Zeta potential of LMP micelles at pH 7.4. Measurement was performed at 1 mg mL^{-1} micelles.*$p \leq 0.05$, **$p \leq 0.01$, ***$p \leq 0.001$. All other comparisons were not significantly different ($p \geq 0.05$).

Pyrene fluorescence was used to characterize the concen- tration at which free block copolymers in solution begin to form micelles. The CMC, shown in Figure 4, was determined for LMP-0, 5, 10, 20, and 30 copolymers to be 73.0, 47.8, 40.6, 41.0, and 32.5 mg L^{-1}, respectively. The slight decreasing trend in CMC with increasing PBA composition can be explained by block copolymer solubility and micelle stability differences. Increasing the PBA composition makes the poly(MAA-co-PBA) block less water-soluble, which reduces the driving force for it to enter into solution. Additionally, the hydrophobic interactions between PBA groups in the corona increase the micelle stability by hindering the dissolution of the micelle's corona. Xue et al. developed poly(D,L-lactide)-b-poly(acrylic acid) micelles of similar molecular weight, which were determined to have a CMC of ~80 mL L^{-1}.[31] This slightly increased CMC may be due to their use of acrylic acid, which is more hydrophilic compared with methacrylic acid.

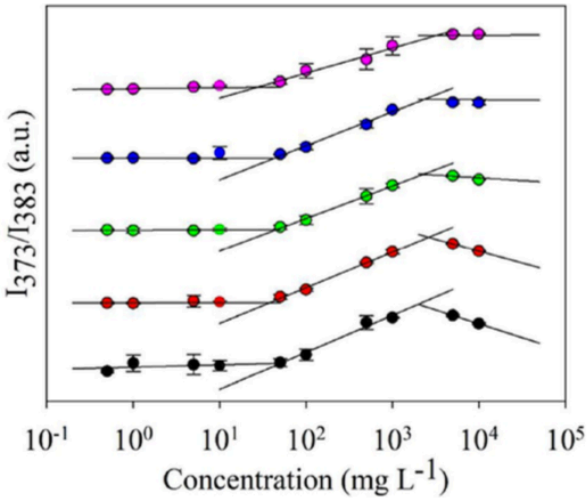

Figure 4. Critical micelle concentration for LMP-0 (black), LMP-5 (red), LMP-10 (green), LMP-20 (blue), and LMP-30 (pink) in 0.1 M PBS pH 7.4 determined from the ratio of fluorescence intensity at 373 to 383 nm after excitation at 340 nm.

Cyclosporine A Release. CycA was entrapped within the LMP micelles by dissolving both components in acetone, followed by the dropwise addition into purified water at a ratio of 20 mg copolymer to 3 mg CycA. Upon evaporation of the acetone under constant stirring for 24 h, the drug-loaded micelles were filtered to determine the % entrapment efficiency (EE). Figure 5a shows the EEs for LMP copolymers as well as a control blank CycA. All LMP micelles showed EEs greater than 99.8% (15 wt % CycA/polymer), while the blank CycA formulation had significantly smaller EE of 98.7% ($p < 0.001$), which represents the maximum solubility of CycA in water. This high EE shows that LMP micelles are very effective in loading CycA, which may reduce the initial undesirable burst release upon application. It also suggests that less LMP copolymer could be used to achieve a desirable loading wt %, although this was not examined in this study. These LMP copolymers also showed significantly higher entrapment than similar pLA-b-dextran-g-PBA micelles developed by Liu et al., which only achieved a 30% EE (11.9 wt % CycA/polymer).[19]

Their low entrapment is likely because of the use of dimethyl sulfoxide to form the micelles, which dissolves a large portion of the CycA and cannot be removed prior to drug release studies. Figure 5b shows the solutions of CycA loaded LMP micelles. While unloaded micelles were visually transparent, it can be seen that LMP-0/5/10 micelles are translucent while the LMP- 20 and LMP-30 loaded micelles form opaque suspensions. This may be due to changes in the distribution of CycA within the micelle that alter its refractive properties. The LMP-0/5/10 micelles likely load the majority of CycA within their hydrophobic poly(D,L-lactide) core and less in the outer hydrophilic MAA-rich corona, resulting in minimal refractive changes. Because of the hydrophobic PBA content in the corona of the LMP-20/30 micelles a significant amount of hydrophobic CycA is able to accumulate here, which may account for the changes in solution opacity.

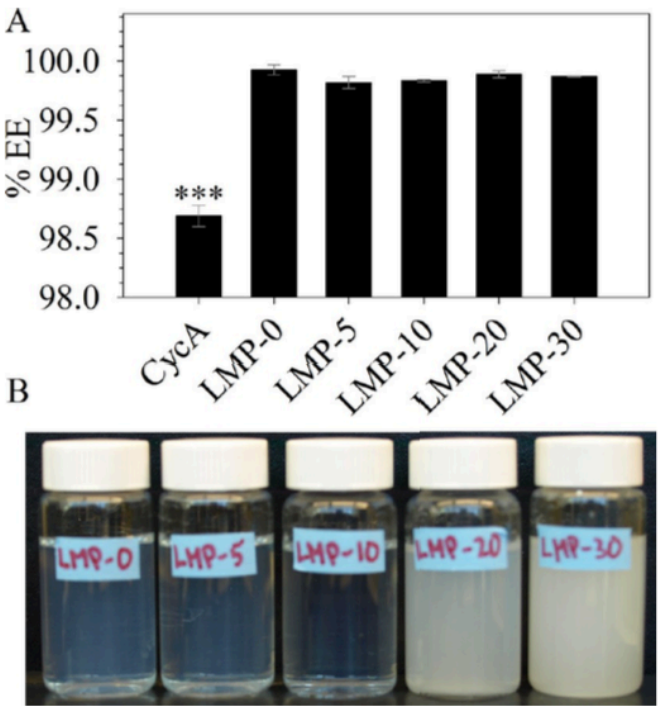

Figure 5. (A) Entrapment efficiencies of LMP copolymers and CycA control. ***$p < 0.001$ compared with all LMP copolymers. All other comparisons were not significant $p > 0.05$. (B) CycA-loaded LMP micelles. LMP-0/5/10 all showed translucent suspensions, while the LMP-20/30 micelles showed opaque stable suspensions.

Interestingly, all LMP copolymers showed faster release compared with free CycA in STF, shown in Figure 6. This increased release is likely due to two main reasons. Free block copolymer is able to diffuse across the 50 kDa MWCO dialysis membrane carrying with it CycA in the hydrophobic poly(D,L- lactide) block, which simulates in vivo conditions where there would be no barriers to individual block copolymer diffusion. Also, the blank CycA formed large-crystal aggregates, which would have a smaller surface area for dissolution compared with the CycA-loaded micelles. All LMP copolymers showed a two- phase release profile characterized by an initial burst phase lasting ~24 h, resulting in between 35 to 45% released, followed by a nonlinear release of between 74 and 80% after 14 days depending on composition. During the initial burst release phase, CycA release was slightly faster from micelles with lower PBA composition, but this trend was reversed over the course of the release. This may be attributed to differences in CycA distribution within the micelle as previously explained. Lower PBA content would result in CycA loading mainly within the hydrophobic poly(D,L-lactide) core, but as PBA content is increased more CycA can be distributed within the corona. In the low PBA materials there is a greater initial driving force for CycA diffusion due to the larger concentration gradient, but this becomes less significant over the course of the release. In the high PBA materials a more homogeneous CycA distribution throughout the micelle will reduce the initial concentration gradient but will increase the diffusivity across the corona due to presence of hydrophobic PBA segments.

This increased diffusivity explains why faster release is seen in the high PBA micelles during the later stage of release. Compared with the poly(lactide)-b-dextran-g-PBA micelles developed by Liu et al., who achieved a 100% release after ~5 days, our release is significantly slower, but as previously explained this is likely due to the use of DMSO, which falsely increases the solubility and release of CycA from these micelles.[19] The evaporation of acetone prior to drug release in our system shows more realistic drug release profiles and is more clinically applicable for material synthesis.

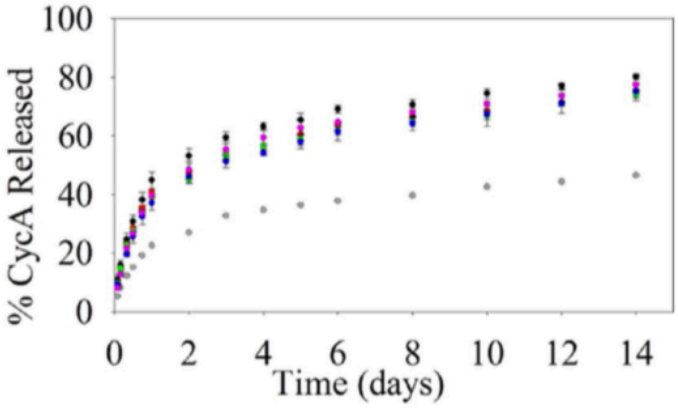

Figure 6. Cumulative CycA release from LMP-0 (black), LMP-5 (red), LMP-10 (green), LMP-20 (blue), LMP-30 (pink), and CycA (gray).

Mucoadhesion. Mucoadhesion of LMP copolymers was studied using SPR with chitosan as a positive control for mucoadhesive comparison. Figure 7 shows the single-angle SPR sensorgram for chitosan and the LMP copolymers. It can be immediately seen from this Figure that mucoadhesion of the LMP micelles increases with increasing PBA content but appears to reach a ceiling whereby additional PBA does not greatly increase mucoadhesion. This ceiling effect may be due to saturation of the mucin monolayer, whereby no additional LMP micelles are able to adhere to the surface, which is representative of in vivo conditions. This suggests that higher PBA compositions may not be significantly more beneficial for clinical outcomes. The LMP-10/20/30 micelles all reached a significantly higher relative intensity compared with the chitosan and the LMP-0/5 micelles, which suggests greater mucoadhesion. The LMP-0 micelles show the lowest mucoadhesion, which was expected. As with chitosan, the LMP-0 micelles also showed a greater reduction in relative intensity after the washing step compared with the PBA containing micelles. This reduction represents the stability of the adsorbed layer.[32] This is likely due to the additional bonding between PBA and sialic acid diols and the hydrophobic interactions between the PBA and hydrophobic segments on the mucin glycoprotein compared with the LMP-0 micelles, which predominately form hydrogen bonds, and chitosan, which predominantly forms electrostatic and hydrogen bonds with mucin. Compared with chitosan, these PBA-containing micelles show excellent in vitro mucoadhesion, which supports their potential to improve bioavailability of topically

applied ophthalmic drugs.

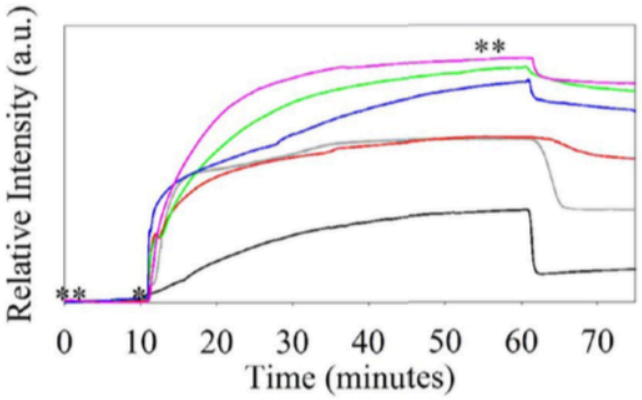

Figure 7. SPR single-angle sensorgram of chitosan (gray), LMP-0 (black), LMP-5 (red), LMP-10 (green), LMP-20 (blue), and LMP-30 (pink) flowing across a mucin adsorbed gold sensor (** = STF, * = LMP micelles or chitosan addition).

HCEC Viability. To test in vitro cell viability, we incubated HCECs with LMP micelles at concentrations of 1 and 5 mg mL^{-1} for 24 and 72 h. At each time point, cell metabolic activity was determined using an MTT assay, and live/dead cell counts were determined using CalAM/EthD-1 assays, respectively. It can been seen from the MTT assay results (Figure 8A) that cell metabolism is reduced compared with controls. It also shows a trend that after 72 h the metabolism of HCECs incubated with 1 mg mL^{-1} micelles is significantly higher than those incubated with 5 mg mL^{-1} micelles. The viability, determined from fluorescent CalAM staining (Figure 8B), showed that viability was higher after 72 h compared with 24 h samples. CalAM fluorescence also showed that viability was higher for 1 mg mL^{-1} micelles compared with the 5 mg mL^{-1} micelles. The EthD-1 assay (Figure 8C) showed less than three times morbidity for all micelles compared with controls, which suggests that LMP micelles are not significantly cytotoxic. The EthD-1 assay also showed a trend that % morbidity was significantly lower after 72 h compared with 24 h, which may be due to control cells reaching confluence, which initiates cell death, while the slower growing HCECs containing micelles had not. Interestingly, Figure 8D–M shows morphological changes in HCEC growth. HCECs cultured with PBA containing micelles show dense clusters of cells rather than even spreading, as seen in the micelles not containing PBA and the controls. The PBA micelles could be mediating cell–cell adhesion by interacting with cell surface mucins, which prevents them from spreading on the plate.[33] It is not believed that inhibition of cell growth seen with these LMP micelles will significantly affect corneal cells in vivo for two reasons: the concentration of LMP micelles on the corneal surface will be lower than those tested due to the rapid tear turnover of a significant portion of topical administration of eye drops, and the anterior layer of corneal cells is not actively dividing so the reduced in vitro proliferation will not likely affect in vivo corneal

viability.[34] The cell viability results show that these PBA-containing micelles are not significantly cytotoxic but do inhibit HCEC growth and cause clustered cell growth.

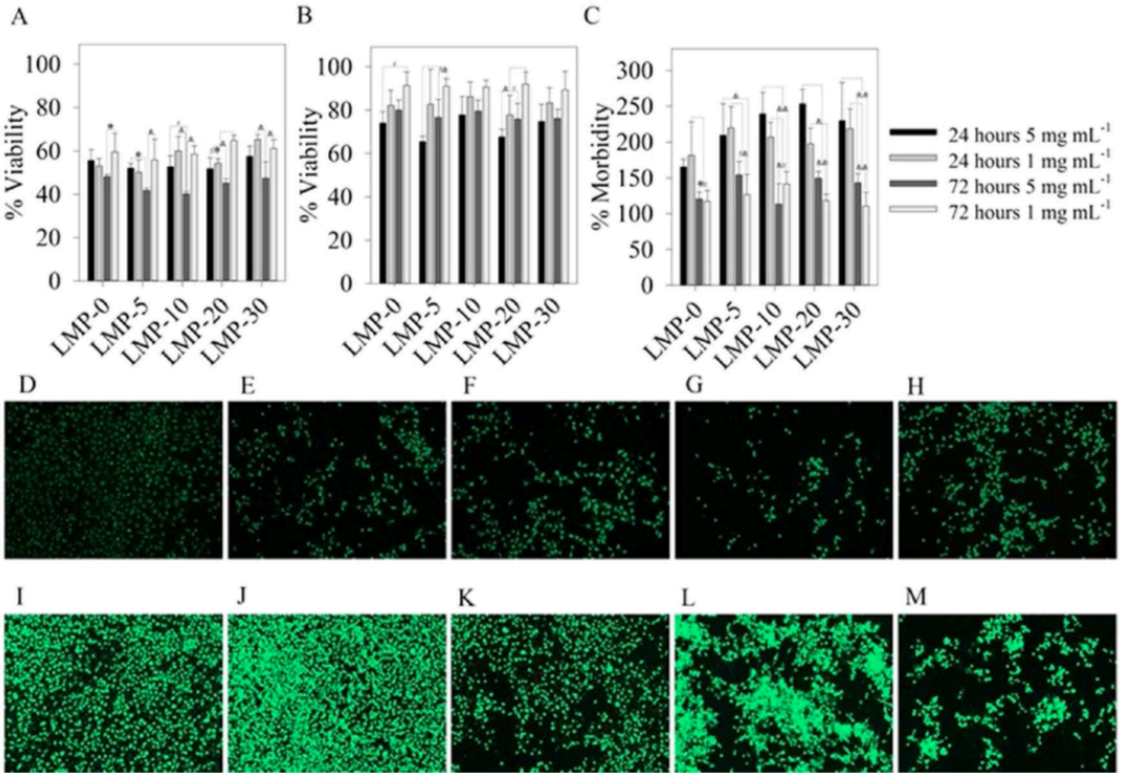

Figure 8. HCEC viability by (A) MTT assay, (B) CalAM, (C) EthD-1, (D) control 24 h, (E) LMP-0 24 h 1 mg mL^{-1}, (F) LMP-0 24 h 5 mg mL^{-1}, (G) LMP-30 24 h 1 mg mL^{-1}, (H) LMP-30 24 h 5 mg mL^{-1}, (I) control 72 h, (J) LMP-0 72 h 1 mg mL^{-1}, (K) LMP-0 72 h 5 mg mL^{-1}, (L) LMP-30 72 h 1 mg mL^{-1}, and (M) LMP-30 72 h 5 mg mL^{-1}. Green = live cells and red = dead cells. * = $p \leq 0.05$, # = $p \leq 0.01$, & = $p \leq 0.001$.

In Vivo Acute Ocular Irritation Testing. The LMP micelle dosage in the acute ocular irritation testing was based on ensuring that a clinically relevant dosage of CycA, similar to Allergan's Restasis of 0.5 mg mL^{-1}, could be achieved. Although a 3.3 mg mL^{-1} micelle solution was shown to achieve >99% entrapment of 0.5 mg mL^{-1} CycA, a 5 mg mL^{-1} LMP copolymer solution was chosen to increase the severity of the irritation challenge and test whether other pharmacologic agents that have lower entrapment efficiencies could be used with this system. Ten μL of 5 mg mL^{-1} micelles was instilled into the right eye of Sprague–Dawley rats to simulate a surface- area-adjusted dosage compared with human eyes. A single daily dosage was used because this technology is hypothesized to reduce the dosage quantity and frequency compared with commercially available Restasis. After 10 days of daily instillation of micelle solution drops into the right eye of Sprague–Dawley rats there was no visible effect on corneal health based on slit lamp microscopy, shown in Figure 9A–D. Corneas remain transparent, healthy, and free from visible hyperemia or inflammation. Fluorescein staining confirms these results, showing a nonfluorescent intact corneal epithelium in Figure 9E–H. OCT was used to study any changes in the corneal cross-sectional thickness or composition. No gross changes in corneal thickness or composition were noted, shown in Figure 9I–L. The

micelles themselves are not visible under microscopy, indicating they did not form aggregates and further demonstrating the ocular biocompatibility of these particles. Overall, these micelles showed excellent biocompatibility on the ocular surface of Sprague–Dawley rats after 10 days of instillation, suggesting their potential to be well tolerated in the human eye.

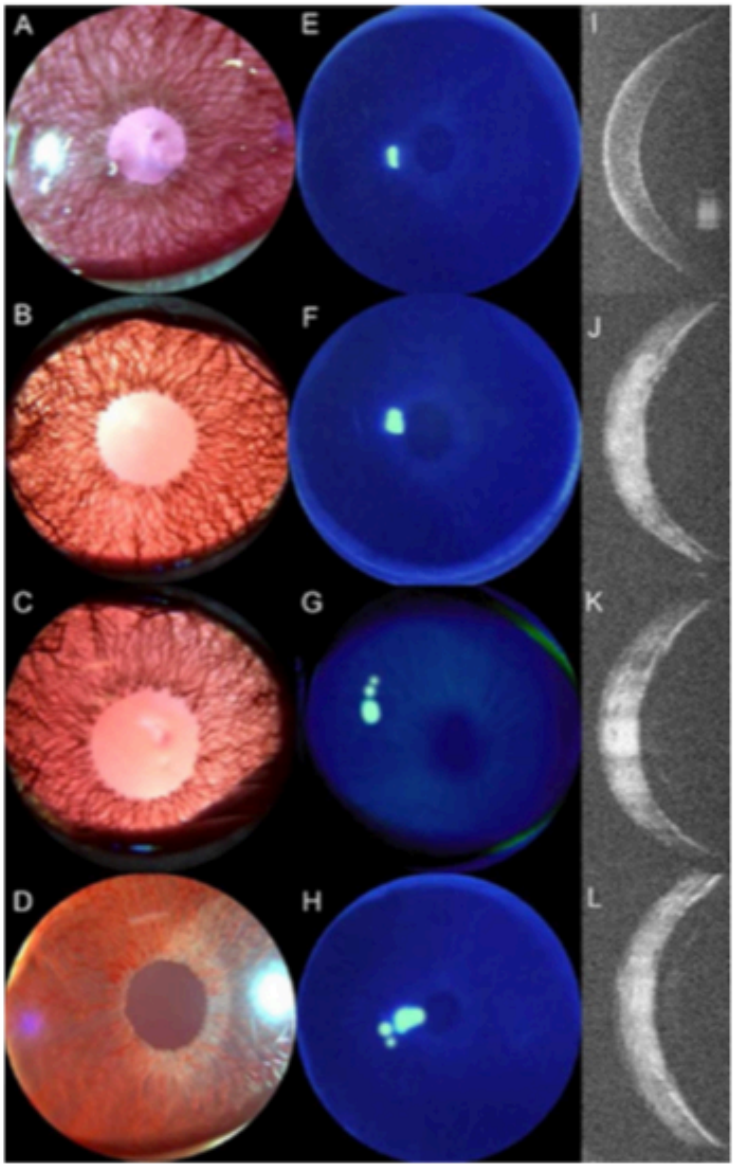

Figure 9. Slit lamp, fluorescence, and OCT images for LMP-0 (A,E,I), LMP-10 (B,F,J), LMP-30 (C,G,K), and negative control (D,H,L).

CONCLUSIONS

Mucoadhesive micelles offer significant potential to increase the bioavailability of topically applied ophthalmic drugs. This will help to decrease the dosage, frequency of dose, and off-target systemic toxicity that are commonly associated with topical pharmacologic drops. We have synthesized a series of poly(L- lactide)-b-poly(methacrylic acid-co-phenylboronic acid) copoly- mer micelles with varying amounts of phenylboronic acid by reversible addition−fragmentation chain-transfer polymeriza- tion. These micelles have shown improved mucoadhesion compared with commonly known mucoadhesive chitosan and have demonstrated the ability to improve the delivery of CycA. In vitro cell viability showed reduced cell proliferation and altered morphology but did not show significant cytotoxicity, which was further proven with in vivo ocular irritation rat model. This method to synthesize mucoadhesive micelles offers significant potential to improve the bioavailability of topically applied drugs to treat anterior segment eye diseases.

Corresponding Author

*Tel: + 1 (905) 525 9140, ext. 24794. E-mail: sheardow@ mcmaster.ca.

Present Address

§ G.P.-P.: Cumming School of Medicine, University of Calgary, 3330 Hospital Drive NW, Calgary, Alberta, Canada T2N 4N1.

Notes

The authors declare no competing financial interests.

ACKNOWLEDGEMENTS

We thank the Natural Sciences and Engineering Research Council (NSERC), and the 20/20 NSERC Ophthalmic Materials Research Network for funding. We also thank Lina Liu and Marion Jamard for their help with TEM, Dr. Emily Cranston for SPR use, Dr. Robert Pelton for ZetaPlus use, Dr. Todd Hoare for HPLC use, and the McMaster Biointerfaces Institute for their equipment use and expertise.

ABBREVIATIONS

AIBN, azobis(isobutyronitrile); CalAM, calcein AM; CMC, critical micelle concentration; CycA, cyclosporine A; DED, dry eye disease; EE, entrapment efficiency; EthD-1, ethidium homodimer-1; DMSO, dimethyl sulfoxide; HCECs, human corneal epithelial cells; HPLC, high-performance liquid chromatography; KSFM, keratinocyte serum-free media; MAA, methacrylic acid; MTT, 3-[4,5-dimethylthiazole-2-yl]- 2,5-diphenyl-tertazolium bromide; OCT, optical coherence tomography; PBA, phenylboronic

acid; PBS, phosphate- buffered saline; pLA-CPD, poly(D,L-lactide) 4-cyano-4-[(dodecylsulfanylthiocarbonyl)sulfanyl]pentoate; TEM, trans- mission electron microscopy

REFERENCES

(1) Shell, J. W. Pharmacokinetics of Topically Applied Ophthalmic Drugs. Surv. Ophthalmol. 1982, 26 (4), 207–218.

(2) Cholkar, K.; Patel, S. P.; Vadlapudi, A. D.; Mitra, A. K. Novel Strategies for Anterior Segment Ocular Drug Delivery. J. Ocul. Pharmacol. Ther. 2013, 29 (2), 106–123.

(3) Mishima, S.; Gasset, A.; Klyce, S. D. J.; Baum, J. L. Determination of Tear Volume and Tear Flow. Invest. Ophthalmol. 1966, 5 (3), 264– 276.

(4) Davidson, H. J.; Kuonen, V. J. The Tear Film and Ocular Mucins. Vet. Ophthalmol. 2004, 7 (2), 71–77.

(5) Ruponen, M.; Urtti, A. Undefined Role of Mucus as a Barrier in Ocular Drug Delivery. Eur. J. Pharm. Biopharm. 2015, 96, 442–446.

(6) Argüeso, P.; Tisdale, A.; Spurr-Michaud, S.; Sumiyoshi, M.; Gipson, I. K. Mucin Characteristics of Human Corneal-Limbal Epithelial Cells That Exclude the Rose Bengal Anionic Dye. Invest. Ophthalmol. Visual Sci. 2006, 47 (1), 113–119.

(7)Goycoolea,F.M.;Lollo,G.;Remuñań-Lopez,C.;Quaglia,F.; Alonso, M. J. Chitosan-Alginate Blended Nanoparticles as Carriers for the Transmucosal Delivery of Macromolecules. Biomacromolecules 2009, 10 (7), 1736–1743.

(8) Sogias, I. a; Williams, A. C.; Khutoryanskiy, V. V. Why Is Chitosan Mucoadhesive? Biomacromolecules 2008, 9 (7), 1837–1842. (9) Menchicchi, B.; Fuenzalida, J. P.; Bobbili, K. B.; Hensel, A.; Swamy, M. J.; Goycoolea, F. M. Structure of Chitosan Determines Its Interactions with Mucin. Biomacromolecules 2014, 15 (10), 3550–

3558. (10) Menchicchi, B.; Fuenzalida, J. P.; Hensel, A.; Swamy, M. J.;

David, L.; Rochas, C.; Goycoolea, F. M. Biophysical Analysis of the Molecular Interactions between Polysaccharides and Mucin. Bio- macromolecules 2015, 16 (3), 924–935.

(11) Pal, D.; Nayak, A. Development, Optimization, and Anti- Diabetic Activity of Gliclazide-Loaded Alginate–Methyl Cellulose Mucoadhesive Microcapsules. AAPS PharmSciTech 2011, 12 (4), 1431–1441.

(12) Dubolazov, A. V.; Nurkeeva, Z. S.; Mun, G. a; Khutoryanskiy, V. V. Design of Mucoadhesive Polymeric Films Based on Blends of Poly(acrylic Acid) and (hydroxypropyl)cellulose. Biomacromolecules 2006, 7 (5), 1637–1643.

(13) Bernkop-Schnürch, A. Thiomers: A New Generation of Mucoadhesive Polymers. Adv. Drug Delivery Rev. 2005, 57 (11), 1569–1582.

(14) Roldo, M.; Hornof, M.; Caliceti, P.; Bernkop-Schnürch, A. Mucoadhesive Thiolated Chitosans as Platforms for Oral Controlled Drug Delivery: Synthesis and in Vitro Evaluation. Eur. J. Pharm. Biopharm. 2004, 57 (1), 115–121.

(15) Springsteen, G.; Wang, B. A Detailed Examination of Boronic Acid-Diol Complexation. Tetrahedron 2002, 58 (26), 5291–5300.

(16) Li, C.; Liu, Z.; Yan, X.; Lu, W.; Liu, Y. Mucin-Controlled Drug Release from Mucoadhesive Phenylboronic Acid-Rich Nanoparticles. Int. J. Pharm. 2015, 479 (1), 261–264.

(17) Cheng, C.; Zhang, X.; Xiang, J.; Wang, Y.; Zheng, C.; Lu, Z.; Li, C. Development of Novel Self-Assembled poly(3-Acrylamidophenyl- boronic acid)/poly(2-Lactobionamidoethyl Methacrylate) Hybrid Nanoparticles for Improving Nasal Adsorption of Insulin. Soft Matter 2012, 8 (3), 765.

(18) Jachowicz, R.; Czech, A. Preparation and Evaluation of Piroxicam-HPMCAS Solid Dispersions for Ocular Use. Pharm. Dev. Technol. 2008, 13 (6), 495–504.

(19) Liu, S.; Jones, L.; Gu, F. X. Development of Mucoadhesive Drug Delivery System Using Phenylboronic Acid Functionalized poly(D,L- Lactide)-B-Dextran Nanoparticles. Macromol. Biosci. 2012, 12 (12), 1622–1626.

(20) Schaumberg, D. A.; Dana, R.; Buring, J. E.; Sullivan, D. A.; Sullivan, a. Prevalence of Dry Eye Disease among US Men: Estimates from the Physicians' Health Studies. Arch. Ophthalmol. 2009, 127 (6), 763–768.

(21) Schaumberg, D. A.; Sullivan, D. A.; Buring, J. E.; Dana, M. R. Prevalence of Dry Eye Syndrome among US Women. Am. J. Ophthalmol. 2003, 136 (2), 318–326.

(22) Schein, O. D.; Munoz, B.; Tielsch, J. M.; Bandeen-Roche, K.; West, S. Prevalence of Dry Eye among the Elderly. Am. J. Ophthalmol. 1997, 124 (6), 723–728.

(23) Schein, O. D.; Hochberg, M. C.; Munoz, B.; Tielsch, J. M.; Bandeen-Roche, K.; Provost, T.; Anhalt, G. J.; West, S. Dry Eye and Dry Mouth in the Elderly: A Population-Based Assessment. Arch. Intern. Med. 1999, 159 (12), 1359–1363.

(24) Gayton, J. L. Etiology, Prevalence, and Treatment of Dry Eye Disease. Clin. Ophthalmol. 2009, 3, 405–412.

(25) Kymionis, G. D.; Bouzoukis, D. I.; Diakonis, V. F.; Siganos, C. Treatment of Chronic Dry Eye: Focus on Cyclosporine. Clin. Ophthalmol. 2008, 2 (4), 829–836.

(26) Kunert, K. S.; Tisdale, A. S.; Stern, M. E.; Smith, J. a; Gipson, I. K. Analysis of Topical Cyclosporine Treatment of Patients with Dry Eye Syndrome: Effect on Conjunctival Lymphocytes. Arch. Oph- thalmol. 2000, 118 (11), 1489–1496.

(27) Stern, M. E.; Gao, J.; Schwalb, T. A.; Ngo, M.; Tieu, D. D.; Chan, C.-C.; Reis, B. L.; Whitcup, S. M.; Thompson, D.; Smith, J. A. Conjunctival T-Cell Subpopulations in Sjogren's and Non-Sjogren's Patients with Dry Eye. Invest. Ophthalmol. Vis. Sci. 2002, 43 (8), 2609–2614.

(28) Kunert, K. S.; Tisdale, A. S.; Gipson, I. K. Goblet Cell Numbers and Epithelial Proliferation in the Conjunctiva of Patients with Dry Eye Syndrome Treated with Cyclosporine. Arch. Ophthalmol. 2002, 120 (3), 330–337.

(29) Aguiar, J.; Carpena, P.; Molina-Bolívar, J. a.; Carnero Ruiz, C. On the Determination of the Critical Micelle Concentration by the Pyrene 1:3 Ratio Method. J. Colloid Interface Sci. 2003, 258 (1), 116– 122.

(30) Fischer, F. H.; Wiederholt, M. Human Precorneal Tear Film pH Measured by Microelectrodes. Graefe's Arch. Clin. Exp. Ophthalmol. 1982, 218 (3), 168–170.

(31) Xue, Y. N.; Huang, Z. Z.; Zhang, J. T.; Liu, M.; Zhang, M.; Huang, S. W.; Zhuo, R. X. Synthesis and Self-Assembly of Amphiphilic Poly(acrylic Acid-B-Dl-Lactide) to Form Micelles for pH-Responsive Drug Delivery. Polymer 2009, 50 (15), 3706–3713.

(32) Bravo-Osuna, I.; Noiray, M.; Briand, E.; Woodward, a M.; Argüeso, P.; Molina Martínez, I. T.; Herrero-Vanrell, R.; Ponchel, G. Interfacial Interaction between Transmembrane Ocular Mucins and Adhesive Polymers and Dendrimers Analyzed by Surface Plasmon Resonance. Pharm. Res. 2012, 29 (8), 2329–2340.

(33) Inatomi, T.; Spurr-Michaud, S.; Tisdale, a. S.; Gipson, I. K. Human Corneal and Conjunctival Epithelia Express MUC1Mucin. Investig. Ophthalmol. Vis. Sci. 1995, 36 (9), 1818–1827.

(34) Thassu, D.; Chader, G. J. Eye Anatomy, Physiology, and Occular Barriers: Basic Considerations for Drug Delivery. In Ocular Drug Delivery Systems: Barriers and Application of Nanoparticulate Systems; CRC Press Taylor & Francis Group, 2013; pp 17–40.